JOM, Vol. 72, No. 11, 2020
https://doi.org/10.1007/s11837-020-04338-7

Effect of Reheating in the Solid–Liquid Region on Al-5Fe-4Cu-Based Alloys

WEI WANG[1] and BO LIU[1,2]

1.—School of Naval Architecture and Electromechanical Engineering, Zhejiang Ocean University, Zhoushan 316022, China. 2.—e-mail: liubo@zjou.edu.cn

Two Al-5Fe-4Cu-based alloys, AF1 alloy and AF15 alloy, with a high-volume fraction of second-phase iron-bearing intermetallics (AlFe phases for short) were reheated to a solid–liquid region, and the microstructural evolution of the alloys was investigated. During heating in the solid–liquid region, the high-melting-point solid AlFe phases were demonstrated to stunt grain growth, block liquid convection, restrict diffusion and coalescence, and reduce movement of solids. This mechanical barrier affected semisolid heating and prompted the formation of grains with increased high-angle grain boundaries (HAGBs), resulting in alloys with smaller grain sizes and lower coarsening rate constants. Consequently, the grains from the earlier stage (5–20 min) of isothermal heating were several times larger than those from the later stage (20–60 min), whereas average diameter of the grains increased with elevated heating temperatures and prolonged holding time. The coarsening of Al-5Fe-4Cu-based alloys is predominantly controlled by grain boundary diffusion. The AF15 alloy had a higher fraction of AlFe phases and more complex phase morphologies than the AF1 alloy. Furthermore, it had coarsening rate constants only one-fifth to one tenth those of the AF1 alloy.

INTRODUCTION

Al-Fe alloys are potential superior lightweight heat- and wear-resistant materials. Furthermore, aluminum and iron combine readily, forming a lamellate or acicular fragile intermetallic phase that causes stress concentrations and degrades the final performance of the products, because the solid solubility of iron in aluminum is insignificant. Therefore, the low-cost manufacture of Al-Fe alloys has become a key factor in determining its potential for wide adoption. Recently, Yuan et al. and Liu et al.[1,2] have produced hypereutectic Al-5Fe-based semisolid alloys. The tensile strength, yield strength and elongation of Al5Fe4Cu2ZnMnMg and Al5Fe4-Cu2CrZnMnMgZr semisolid alloys at 298 K, 473 K, 523 K, and 573 K were 308 MPa, 266 MPa, and 1.6%, 246 MPa, 171 MPa and 2.1%, 210 MPa, 165 MPa and 3.1%, and 158 MPa, 139 MPa and 6.1% for the Al5Fe4Cu2ZnMnMg alloy; and 290 MPa, 269 MPa and 1%, 241 MPa, 209 MPa and 0.95%, 201 MPa, 179 MPa and 1.1%, and 157 MPa, 135 MPa and 1.6% for the Al5Fe4-Cu2CrZnMnMgZr alloy, respectively.[2] The tensile strength and elongation of the Al17Si5Fe4-Cu3Mn1Mg semisolid alloy reached 254 MPa and 1.7% at 298 K, and also exceeded 200 MPa and 2.8% at 423 K, respectively.[1] The weight loss of Al17Si5-Fe4Cu3Mn1MgTi alloy after loading for 70 min was only 30.8% that of the 390 Al alloy under dry friction conditions at 423 K. Under lubrication at 423 K, the average wear loss of samples was 1.77 mg, which was only 3.1% that of the 390 Al alloy.[3] Al-Fe-based semisolid alloys not only have better mechanical properties at room temperature and at high temperature, but also have better heat resistance and wear resistance. These studies demonstrated that the semisolid is an effective and inexpensive approach for making this alloy containing a high-volume fraction second phase.

Heating aluminum alloys in the solid–liquid region stimulates grain coarsening, as a result of migrating grain boundary liquid films, with the coarsening rate related to the solid volume fraction. Furthermore, the coarsening rate increases with an

(Received June 6, 2020; accepted August 17, 2020; published online September 8, 2020)

increase in the solid fraction before reaching a critical value and then decreases over this critical value.[4,5] During this process, the isolated, not wetted, and larger granules, as well as the thermally stable dispersoid in the alloys (dispersoids larger than the thickness of the grain boundary liquid films), either drag along or pin to migrating grain boundary liquid films, or inhibit the liquid diffusing from one boundary position to another. The insoluble particles containing iron and manganese in the cooling slopes of cast 2014 alloy and cast 319 alloy were proven to be more effective barriers to migration of the liquid boundary than the soluble Al_2Cu particles that are submicron in size and dissolve below the solidus.[6–8] The second phase decreased the coarsening rate constant in the classic LSW equation.[6] Moreover, the grains with more high-angle grain boundaries (HAGBs) in semisolid alloys had a lower coarsening rate constant, consequently, the fraction of HAGBs could have an influence on the coarsening behavior of semisolid alloys.[9]

A nondendritic microstructure was formed by equiaxed particles of α-Al well insulated from each other by a continuous layer of eutectic liquid during semisolid heating.[10] The structural evolution resulted from the initial melting of the eutectic boundaries between the primary grains, which then penetrated the polygon boundaries, leading to the separation of the initial grains into small new grains.[10–12] Subsequently, solid–liquid interfacial tension made the grains transform into globular or near-globular shapes.[11–13] Spherical grains developed or agglomerated into larger and more irregular shapes.

The initial α-Al phases were quickly coarsened by connecting the secondary arms of the rosette or fine initial α-Al phases when there was a small quantity of the liquid, and slowly coarsened through diffusion when a considerable quantity of the liquid was introduced.[14,15] The coarse solids in aluminum alloys, such as silicon of the extruded Al-Si-Mg alloy and an iron-rich phase in the 7075 alloy, inhibited coarsening or grain rotation during semisolid soaking.[10,16] The coarsening was controlled by the migration rate of liquid films.[10]

The microstructure of the hypereutectic Al-Fe-based alloy in the liquid–solid region included numerous infusible lamellate and blocky AlFe phases with or without other elements, spheroids of α-Al solid, and liquid matrix.[2,17] The heating in the solid–liquid region could make the cusps of acicular iron-rich phases blunter and the longer AlFe phases were divided into several segments as a result of dissolving. Furthermore, the grains tended toward rounding before thixoforming, which had a strong crushing and thinning effect on the solid in the semisolid slurry, especially on the brittle AlFe phases.[18,19] However, there are few studies on the evolution of microstructure during semisolid heating for this type of aluminum alloy. The behavior of the alloys in the solid–liquid region has a significant impact on their properties; accordingly, it is necessary to understand and to recognize this behavior. This investigation researched the microstructure evolution of Al-5Fe-4Cu-based alloys during heating in the solid–liquid region in detail, and we discuss the roles of the AlFe phases on grain coarsening in the semisolid state.

EXPERIMENTS

Two Al-5Fe-4Cu-based alloys were prepared for the semisolid reheating test and abbreviated as AF1 alloy and AF15 alloy, respectively. Their chemical compositions were analyzed by a SPECTROLASB M12 x-ray fluorescence spectrometer and are listed in Table I. The alloys were melted using a 30-kW electrical resistance furnace while controlling the temperature automatically using a black-lead crucible, and the smelting temperature range was from 750°C to 950°C. The alloy billets were prepared by electromagnetic stirring. The material preparation process is described in detail in Ref. 2. The solid–liquid regions of the alloys were measured by differential thermal analysis and were 505.2–649.9°C for the AF1 alloy, and 510.6–662.8°C for the AF15 alloy, respectively. The DSC tests were

Table I. Chemical composition of electromagnetic stirred Al-5Fe-4Cu based alloys' billets (wt.%)

Billet	Fe	Cu	Zn	Cr	Mn	Mg	Zr	Ti	B	Al
AF1-#1	5.83	3.97	2.04	–	0.43	0.34	0.052	0.10	0.01	Bal.
AF1-#2	5.32	4.13	1.57	–	0.39	0.42	0.061	0.096	0.0093	Bal.
AF1-#3	4.76	3.82	2.13	–	0.45	0.40	0.059	0.11	0.01	Bal.
AF1-#4	5.71	4.08	1.84	–	0.56	0.46	0.049	0.093	0.0086	Bal.
AF15-#1	4.89	4.23	0.66	1.81	0.57	0.42	0.35	0.088	0.0076	Bal.
AF15-#2	5.47	4.25	0.61	2.03	0.54	0.34	0.32	0.12	0.01	Bal.
AF15-#3	5.26	4.17	1.56	1.92	0.61	0.46	0.29	0.10	0.0096	Bal.
AF15-#4	5.04	4.09	0.72	2.11	0.53	0.37	0.25	0.11	0.0087	Bal.

carried out using a TA Q100 differential scanning calorimeter; the samples were heated to 900°C at 10°C/min and cooled to room temperature at the same rate. The liquid fraction, the average grain size, and the shape factor (representing the circularity of grains, abbreviated as CF) of the grains were measured by an OLYMPUS BX60M optical microscope with an ISA-4 image analyzer system. The equivalent (average) diameter and CF of the grains were calculated by applying Eqs. 1 and 2.[20]

$$D = \frac{\sum_{i=1}^{N} \sqrt{\frac{4A_i}{\pi}}}{N} \quad (1)$$

$$\mathrm{CF} = \frac{\sum_{i=1}^{N} \frac{4\pi A_i}{P_i^2}}{N} \quad (2)$$

where D, CF, A, N, and P are equivalent diameter, shape factor, area, quantity, and perimeter of the solid particles, respectively. The grain size of each sample was measured as the average of observing ten different fields, each with over five grains. The reheating specimens were cut from 4 billets for each alloy using a digital control wire-electrode cutter and then machined into cylinders with a diameter of 10 mm and a height of 12 mm: these specimens were deliberately unmarked and were chosen for each reheating condition randomly (the schematic diagram of wire electrode cutting of a billet showed in the supplementary material). The specimens were heated in a KOYO-52878 box-type resistance furnace and held for different times after warming at the scheduled temperature and then quenched in cold water. The samples were etched using Keller's reagent. The microstructure was observed using an OLYMPUS BX60M optical microscope and HITACHI S3400n scanning electron microscope.

RESULTS AND DISCUSSION

Effect of Heating in the Solid–Liquid Region on Grain Size

Figure 1 describes the microstructure of the AF1 alloy quenched in cold water after heating in the solid–liquid region for 30 min at different temperatures. The grain sizes in the alloy consisted primarily of sizes between 70 μm and 140 μm accounting for under 50% of the composition at lower heating temperatures and nearer 70% at higher holding temperatures. The smaller grains, under 70 μm, accounted for over 30%, and the larger grains, between 140 μm and 200 μm, accounted for approximately 20% of the composition; there were also a few grains greater than 200 μm (Table II) at a lower heating temperature. The number of the smallest grains ≤ 50 μm diminished rapidly from 12.5% to 2.9%, and the smaller grains 51–70 μm (> 50 μm and ≤ 70 μm) decreased from 18.9% to 10.2%, whereas the middle grains ranging from 71 μm to 140 μm (> 70 μm and ≤ 140 μm) gradually increased from more than 20% to over 30%. Furthermore, the percentage of the larger grains (> 140 μm and ≤ 200 μm) decreased slowly, while the percentage of the largest grains (> 200 μm) were almost invariable with increasing temperature (Table II).

As illustrated in Table II,the grain sizes in the AF15 alloy were distributed mainly between those greater than 50 μm and those smaller than 140 μm, accounting for approximately 80% of the composition at a lower temperature and above 80% at a higher temperature. The number of smaller grains (51–70 μm) decreased from over 20% to the tens, those of the middle grains (> 100 μm and ≤ 140 μm) increased from 15.6% to more than 30%, and the grains in the range 71–100 μm altered insignificantly with increasing temperature. The percentage of larger grains (141–200 μm) in the AF15 alloy was less than 10%: only half that of the AF1 alloy, and this changed little during all heating regimes in the solid–liquid region. The number of the smallest grains (≤ 50 μm) went from tens to single digits with increasing temperature. There were few largest grains in the AF15 alloy, in line with the AF1 alloy, indicating that the vast majority of the grain diameters in Al-5Fe-4Cu-based alloys were less than 200 μm during heating in the solid–liquid region.

The water-quenched microstructure of the AF1 alloy heated at 630°C for different holding times is shown in Fig. 2. The percentage of the grains larger than 50 μm and smaller than 100 μm decreased significantly, and the large grains (> 100 μm and ≤ 200 μm) increased gradually. There were a few of the largest grains (> 200 μm) and the smallest grains (≤ 50 μm), and their numbers remained almost unchanged as the holding time lengthened (Table III); however, the average grain sizes of the alloy increased with increasing holding time. Most of the grain sizes in the AF1 alloy were between 70 μm and 140 μm, accounting for over 60% of all the grains. The smaller grains grew into large grains, but did not develop further into the larger grains, although the average grain size in the alloy increased with increasing heating temperature or holding time, indicating that there were obstructions in the alloys that impeded or restrained the grains from developing further.

Most of the grains in the AF15 alloy were greater than 50 μm and less than 140 μm, accounting for over 80% of all the grains (Table III). The percentage of grains larger than 70 μm and smaller than 140 μm increased gradually and the smaller grains (51–70 μm) decreased gradually with extending holding time. The larger grains (141–200 μm) altered insignificantly and the smallest grains (≤ 50 μm) diminished with increasing holding time, while there were few largest grains (> 200 μm) in the AF15 alloy during holding at 630°C. Accordingly, these changes were different to those of the AF1 alloy.

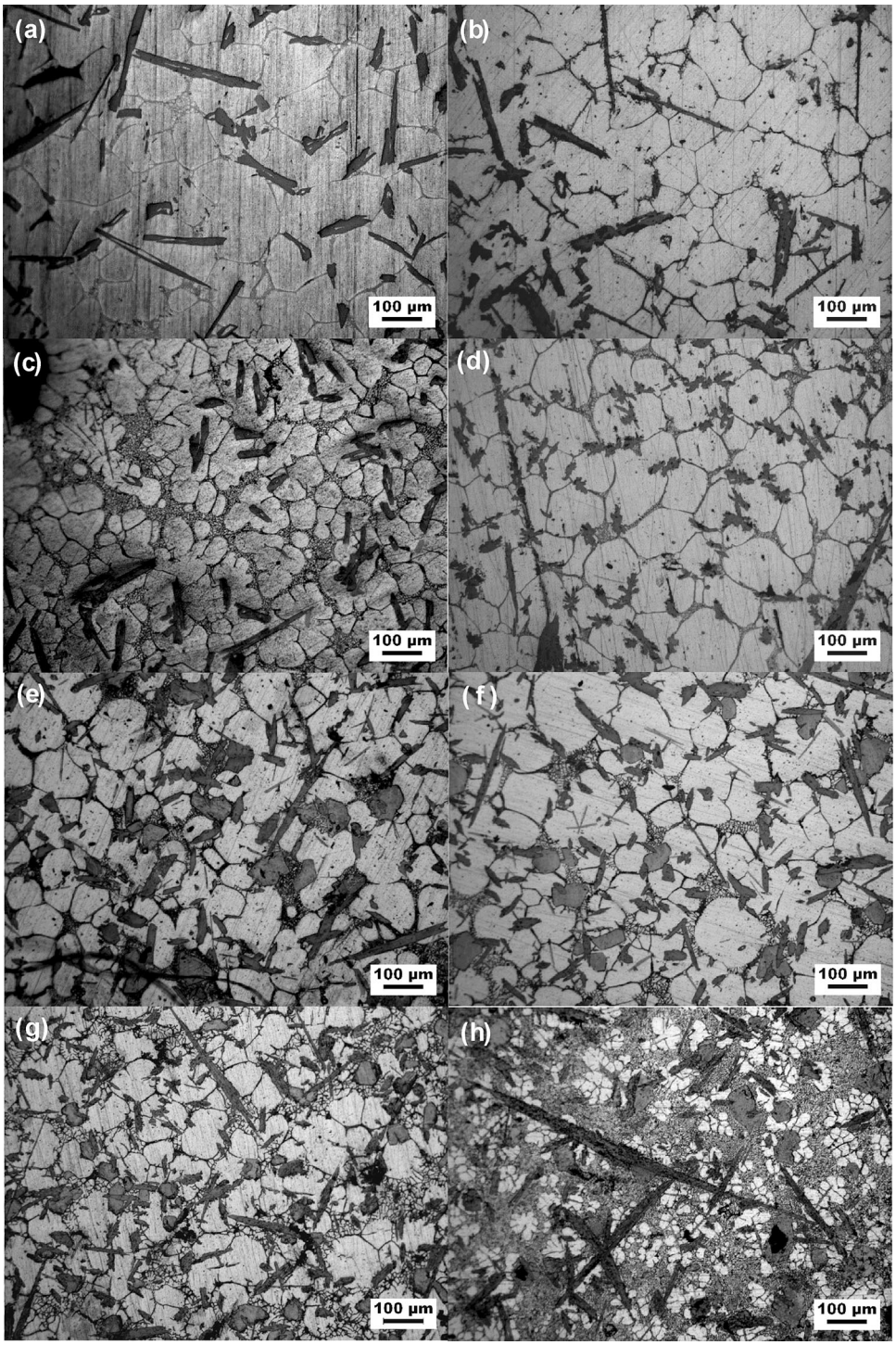

Fig. 1. Water quenched microstructure of the isothermal holding 30 min at 610°C (a), 620°C (b), 630°C (c), and 640°C (d) for AF1 alloy, and at 620°C (e), 630°C (f), 640°C (g), and 650°C (h) for AF15 alloy.

There is a difference in grain size distribution between Tables II and III. This may be related to the following reasons: (1) the specimens under the same conditions derived from different billets for each alloy; (2) the distribution of AlFe phases presented sparsely or densely in a field of view; (3) the fields of view chosen were different; (4) the grains selected were different and so on. Of course, it would be beneficial to reduce this deviation by using specimens of the same or similar composition and microstructure as much as possible, choosing more fields of view in a specimen and selecting more grains in a field and so on. This does indicate that the distribution of the remolten liquid zones in the

Table II. The grains sizes in AF1 alloy and AF15 alloy heated at 30 min for different temperature

		The percent composition of various grain size in the alloy (%)					
Alloy	**Reheating temperature**	**≤ 50 μm**	**51–70 μm**	**71–100 μm**	**101–140 μm**	**141–200 μm**	**> 200 μm**
AF1	610°C	12.46	18.93	25.39	23.82	19.40	0
	620°C	11.43	17.14	28.57	22.86	20.00	0
	630°C	8.86	13.92	29.12	26.58	17.72	3.80
	640°C	2.86	10.21	33.53	36.09	17.31	0
AF15	620°C	11.43	27.59	36.19	15.59	9.20	0
	630°C	14.16	13.79	34.18	28.49	8.37	1.01
	640°C	16.73	12.65	28.42	39.31	2.89	0
	650°C	6.41	19.10	36.67	30.26	7.56	0

alloys is not uniform due to the presence of AlFe phases, resulting in grains that are not uniform in size or shape. However, this does not change the trend of the grain sizes increasing with the elevation of heating temperature or the extension of holding time.

Evolution of the Shape Factor and the Equivalent Diameter in Semisolid Heating

Figure 3 illustrates the change in the shape factor (CF) and the average grain size (D, equivalent diameter) of Al-5Fe-4Cu-based alloys as a function of the heating temperature and the holding time during reheating in the solid–liquid region. With increasing temperature, the average grain sizes of the alloys grew gradually, as the average diameter of the grains increased relatively quickly at first and then slowed with prolonged holding time during semisolid heating. The equivalent diameter of the grains in the AF15 alloy was significantly less than that in the AF1 alloy.

The shapes of the solid particles in the alloys became more globular; however, the CFs decreased quickly after reaching a maximum value with either elevating the temperature or lengthening the holding time (Fig. 3a and c). The CF is an important parameter for thixoforming because it strongly influenced the flowability and the viscosity of the material. Generally, a suitable lengthening of the holding time or elevation of heating temperature in the liquid–solid region was conducive to rounding the grains further. With increased heating temperature and holding time, the liquid soaking led to increased grain circularity or globularity. For ideal round or globular grains, the CF equals 1. When the heating temperature increased from 610°C to 630°C, the CF of the grains increased from 0.80 to 0.82 for the AF1 alloy, and the CF of the AF15 alloy increased from 0.87 to 0.89 with elevating the heating temperature from 620°C to 630°C, indicating that the primary solids became more orbicular. Subsequently, the CFs of the alloys decreased with increasing heating temperature. When heating at 630°C, the CF of the grains in the AF1 alloy increased with increasing holding time, indicating that their shapes became more globular. The CF reached a maximum value at 40 min, which was the best globularity in a semisolid slurry. Subsequently, the CF decreased significantly with increasing holding time, resulting in the formation of larger grains with irregular shape and deteriorating the globularity of the solid grains. For the AF15 alloy, the CF value first increased slowly and achieved maximum values, and then decreased gradually with lengthening holding time at a constant temperature. The CF of the AF15 alloy was better than that of the AF1 alloy. The study confirmed an ideal combination of heating temperature and holding time as the optimum parameters for Al-5Fe-4Cu-based alloys during reheating in the solid–liquid region. Heating between 625°C and 635°C for 20 to 40 min was best for subsequent thixoforming of Al-5Fe-4Cu-based alloys.

Additionally, with increasing temperature, the grains gradually became rounder and were more orbicular in the reheated alloy than that in the electromagnetically stirred alloy[2]; however, the grains did not develop further and the equivalent diameter of the grains increased slightly. When heating at 630°C, the grains coarsened rapidly in the initial stage (up to 20 min), followed by developing slightly with extending holding time, as there was a distinctive inflection point, indicating two different coarsening velocities.

Grain Coarsening During Heating in the Solid–Liquid Region

Grain coarsening is primarily a lattice diffusion-controlled process during heating in the solid–liquid region,[7,13–15] which affects the average grain size of the solid grains in the alloys.[21] Diffusion-controlled coarsening follows the Lifshitz, Slyozov, and Wagner (LSW) equation[22]:

$$D^n - D_0^n = Kt$$

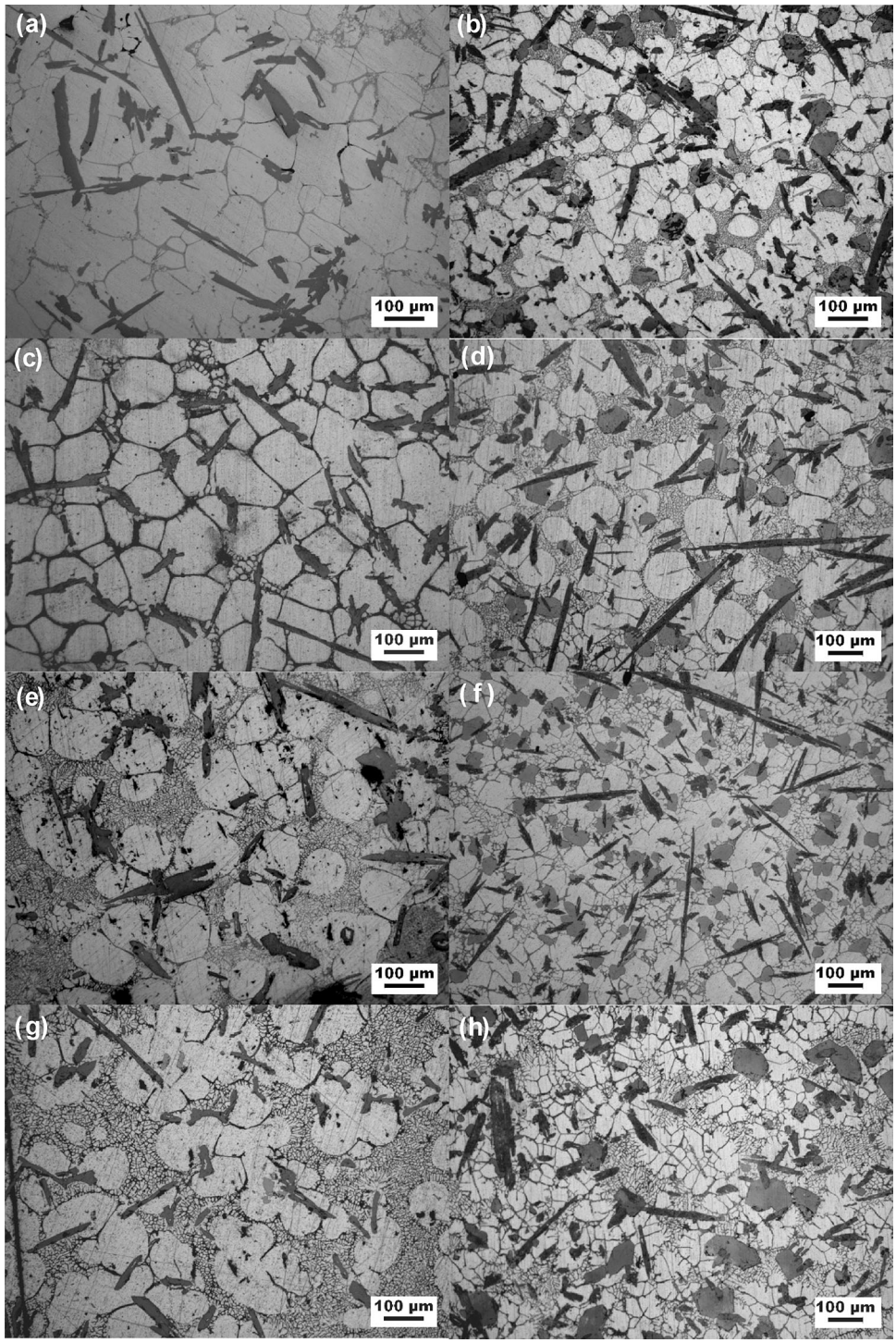

Fig. 2. Water quenched microstructure of AF1 alloy and AF15 alloy reheated at 630°C for 5 min (a) and (b), for 20 min (c) and (d), for 40 min (e) and (f), and for 60 min (g) and (h), respectively.

where t is the isothermal holding time, D is the grain size after time t, D_0 is the initial grain size, K is a coarsening rate constant, and n is the power exponent. In general, n was 2, 3, or 4, representing an interfacial reaction-controlled coarsening, a volume diffusion-controlled coarsening, and a grain boundary diffusion-controlled coarsening, respectively.[23] Although the coarsening kinetics of semisolid alloys has been a controversial problem, the average diameter (D) of the grains in the various alloys after time t at the elevated temperature confirmed the classical LSW equation, and the power exponent was near 3, though varying between 2 and 4 during semisolid heating.[1,6,7,14,15]

Table III. The grains' distribution in Al-5Fe-4Cu based alloys heated at 630°C for various holding times

		The percent composition of various grain size in the alloy (%)					
Alloy	**Holding time (min)**	**≤ 50 μm**	**51–70 μm**	**71–100 μm**	**101–140 μm**	**141–200 μm**	**> 200 μm**
AF1	5	1.59	14.30	31.75	34.90	15.87	1.59
	10	1.32	5.26	34.21	47.37	11.84	0
	15	1.43	4.29	24.28	45.71	21.43	2.86
	20	1.32	1.32	27.63	38.16	30.26	1.31
	40	1.23	3.70	12.35	49.38	33.34	0
	60	0	6.89	18.97	48.28	22.41	3.45
AF15	5	16.65	28.79	25.96	23.98	4.62	0
	10	4.55	23.45	33.56	31.11	7.33	0
	15	5.58	11.86	34.14	38.17	10.25	0
	20	11.0	20.43	39.84	27.02	1.14	0.57
	40	8.79	28.73	42.43	14.84	5.21	0
	60	1.14	16.79	42.68	34.85	4.55	0

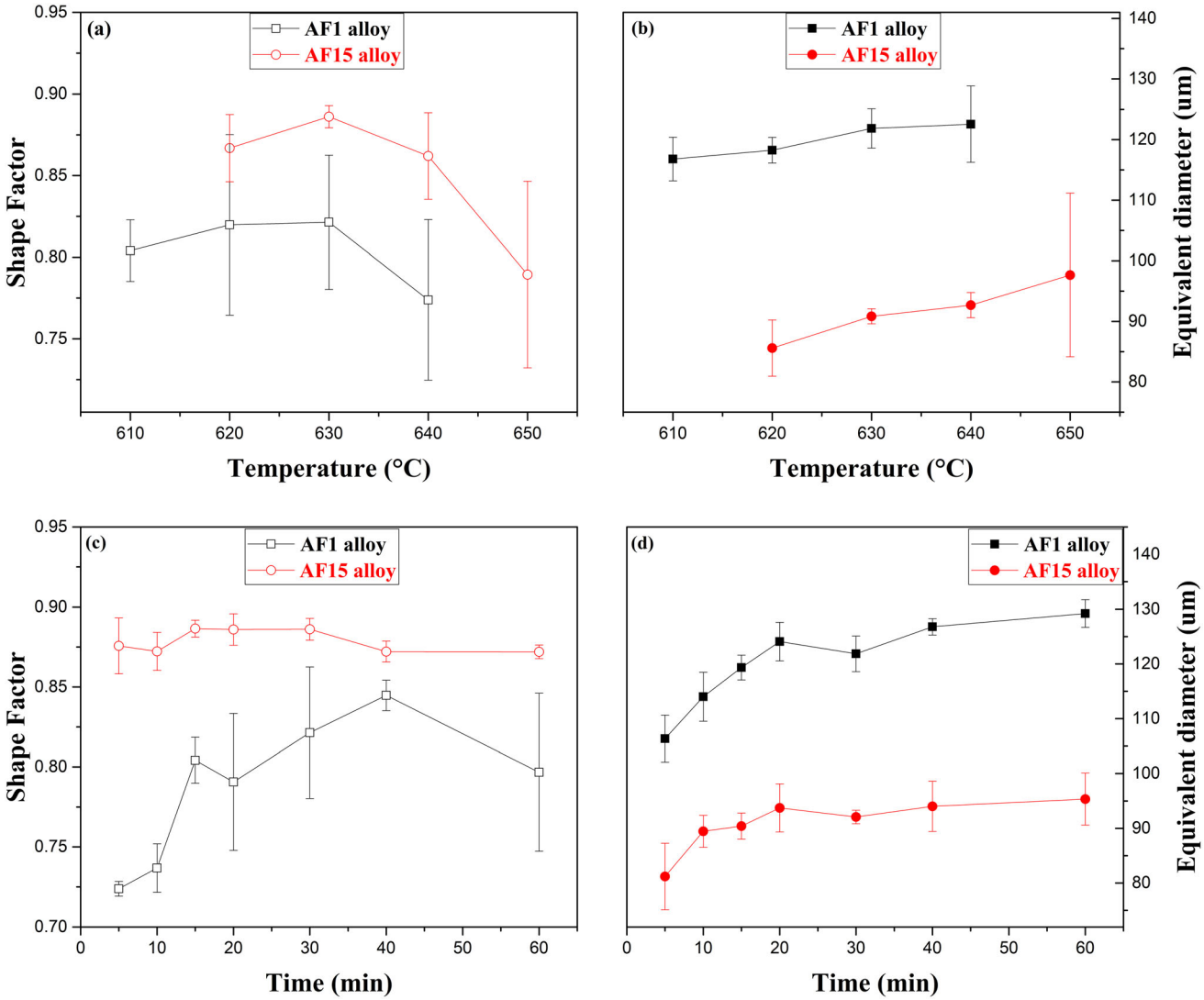

Fig. 3. The shape factor and the equivalent diameter of the grains in Al-5Fe-4Cu-based alloys varied with temperatures, (a) and (b) and with times, (c) and (d), respectively.

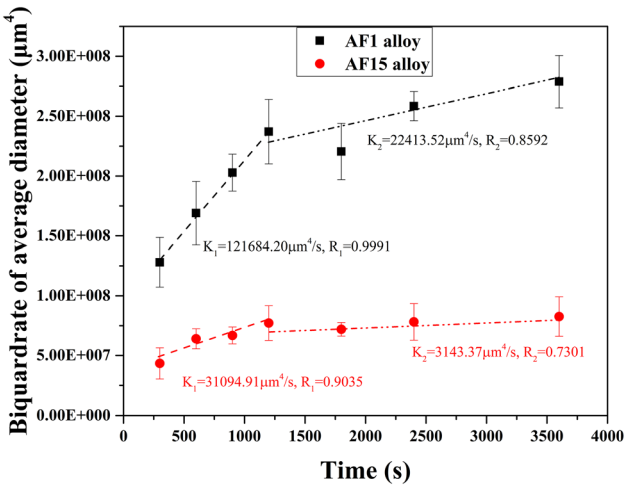

Fig. 4. Plot of relationship between third power of average diameter of the grains and holding time for Al-5Fe-4Cu alloys heated at 630°C, Lines represent the linear fitted to the data. *R* is Pearson regression coefficient and *K* is coarsening rate constant.

Coarsening data for the AF1 alloy and the AF15 alloy during semisolid heating at 630°C are fitted by various power exponents n according to the LSW equation. The best Pearson's coefficients, R, for best linear fits to the data, are acquired when $n = 4$, indicating that the coarsening mechanism of AF1 and AF15 alloys is a grain boundary diffusion-controlled coarsening. Figure 4 plots the coarsening of Al-5Fe-4Cu-based alloys heating at 630°C for various holding times and power exponent $n = 4$. As shown in Fig. 4, there were two coarsening rate constants obtained for each of the alloys, indicating diverse growing rates in the different time regions during heating in the liquid–solid region. With lengthening holding time, the grains first grew rapidly and then gently after reaching an inflection point, implying that the grain growth was hindered by AlFe phases. The coarsening rate constants for the earlier stage (5–20 min) and the later stage (20–60 min) of heating at 630°C were determined to be, K_1 of 121,684.20 $\mu m^4/s$ and K_2 of 22,413.52 $\mu m^4/s$ for the AF1 alloy, and K_1 of 31,094.91 $\mu m^4/s$ and K_2 of 3143.37 $\mu m^4/s$ for the AF15 alloy, respectively. The K value in the earlier stage far surpassed that in the later stage for Al-5Fe-4Cu-based alloys, and the K values of the AF1 alloy were several times larger than those of the AF15 alloy. K was a function of several material properties and corresponded to the speed of the grain coarsening. K generally increased with increasing the heating temperature and the liquid fraction in the liquid–solid region.[7,9,16] This was not only because of faster diffusion at a higher temperature, but the larger liquid fraction also provided more diffusible paths, as the diffusion in the liquid was faster than that in the solid.[16] Once a continuous liquid path was present around the grain, coarsening could accelerate. The liquid fraction of the AF1 alloy increased with soaking time from 12% (5 min) to 27% (20 min) during heating at 630°C,[2] which verged on the equilibrium value of the liquid fraction at this temperature. Hence, the higher K value in the earlier stage of soaking was mainly attributed to the liquid fraction increase with an increase in holding time at the given temperature. The decrease in K value was also ascribed to the obstruction by AlFe phases to the liquid migrating and the rotation of solids, causing grain growth to decelerate or even cease, although the liquid was near saturated in the later stage of heating.

Effect of the AlFe Second Phases on Grain Growth

Figures 1 and 2 illustrate the as-reheated microstructure of the Al-5Fe-4Cu-based alloys. Generally, the microstructure of the alloys was composed of Al nondendrites, iron-bearing intermetallics (AlFe phases), and the liquid in the solid–liquid region. However, the morphology of the AlFe phases varied with the alloy composition. The elongated and flaky AlFe phase was dominant for the AF1 alloy. With the combined additions of chromium and zirconium in the AF15 alloy, a certain number of blocky and ring-like AlFe compounds with chromium and a small quantity of the acicular Al_3Zr intermetallics, with or without titanium, appeared.[19] The infusible AlFe phases in Al-5Fe-4Cu-based alloys were distributed randomly throughout the matrix. The characterization results of the flaky and the blocky AlFe phases from image analysis showed that the average length of the flaky phase was approximately 121 μm for the AF1 alloy and 148 μm in the AF15 alloy. As the length of the phase was referred to as the maximum length from all the directions of the phases, and considering that the AlFe phases were solid throughout semisolid heating, the dimensional characteristics of AlFe phases were calculated at all experimental temperatures. Because the cusps and sides of the elongated and flaky AlFe phases would melt or dissolve partially, and due to the local melting of some longer AlFe phases during heating in the solid–liquid region,[2,19] the average length of AlFe phases in the reheated alloy was distinctly shorter than in the original electromagnetically stirred alloy. In the AF1 alloy, the average length of the sheet AlFe phases was equivalent to the average diameter of the grains, which was approximately 120 μm, but the number of AlFe phases with a length greater than 200 μm exceeded 10%. However, the average length of the flaky AlFe phases in the AF15 alloy exceeded the grain size. For the elongated and flaky AlFe phases, the average areal percentage of the phases in the AF1 alloy was 11.21%, whereas it increased to approximately 14.24% in the AF15 alloy. Due to the addition of chromium into the AF15 alloy resulting in the formation of blocky AlFe phases, the average length of the blocky phases was

approximately 65 μm and the average areal percentage was 8.67%. There were few blocky phases in the AF1 alloy: the lumps on the metallograph were cross-sections of the flaky AlFe phases.

During heating in the solid–liquid region, the Al-5Fe-4Cu-based alloy matrix was randomly divided into many microregions by the insoluble AlFe phases. The liquid in each microregion had different convective and diffusive states; accordingly, the flaky AlFe phase could block the liquid flow while the blocky phase increased the resistance of the fluid, acting like a dam or a reef, respectively. Here, it was assumed that the solid grains in the alloys were a rigid spheres with diameter 2R, the aspect ratio of the flaky AlFe phase was approximately 5:1, and the blocky phase was approximately 2:1. In an ideal state, all the phases would be distributed uniformly. For the AF1 alloy, the average diameter of the solid grain was similar to the average length of the elongated and flaky AlFe phase, and the average area ratio of the grain to the flaky AlFe phase was approximately 3.93. The solid fraction was approximately 67% when heating at 630°C for 30 min, while the flaky AlFe phase was 11.21%, and the solid grain was 55.79%. The number ratio of the solid grains to the flaky AlFe phases per unit volume (area) was approximately 9:7. Generally, AlFe phases in the alloys tended to form star-shaped twin structures, the stellate arms broken into elongated and flake-shaped morphology during electromagnetic stirring and subsequent reheating, resulting in an uneven distribution of the flaky AlFe phase and generating crowded or sparse regions in the different locations. The number ratio of the solid grains to the flaky AlFe phases per unit volume (area) was much less or much higher than 9:7. The smaller this number ratio, the greater the segregation of the flaky AlFe phases. In these microregions, the grains were separated by lamellate phases, and the grain growth was hindered by the lamellae. The partial periphery of the solid grain had liquid which hindered convection between the liquid phases for solute diffusion. The liquid-filled periphery of the grain grew into an arc and the non-liquid periphery grew along the flaky side, resulting in the formation of irregular grains. Moreover, the larger the number ratio, the sparser the distribution of the flaky AlFe phases became. At this point, the grain was filled with the liquid that was partially connected. More precisely, the liquid in the partially molten pools could convect and diffuse mutually, and the components of the liquid in each molten pool were not uniform. The grains grew toward the liquid, and the grain growth was blocked by the flaky AlFe phases encountered. Furthermore, in the non-flaky AlFe phase region, the grain was completely surrounded by the interconnected liquid, and convection and diffusion tended to cause the components of the liquid in the microregion to balance. The grains grew up uniformly and became larger and relatively more rounded in shape. Consequently, this reflected in the shape factor of the AF1 alloy, which fluctuated considerably during heating in the solid–liquid region.

In the AF15 alloy, the average length of the lamellate AlFe phases was significantly longer than the average diameter of the solid grains and the average length of the blocky phases was only approximately two-thirds of the average grain diameter, as there were more AlFe phase systems and more complex morphology. When the AF15 alloy was heated at 630°C for 30 min, the ratio of the solid grains to the flaky AlFe phases per unit volume (area) was approximately 8:9, while the ratio of the solid grains to the blocky phases was approximately 4:1 and the solid grains to the flaky and the blocky phases was approximately 8:11, implying that the distribution of the flaky phases around the grains was significantly denser than that in the AF1 alloy (Figs. 1e, f, g, h, and 2b, d, f, h). Unfortunately, the distribution of AlFe phases in the AF15 alloy did not reach the ideal state, as there were also the crowded regions where the flaky AlFe phase interlaced with the blocky phase to grow. Furthermore, there were sparse regions of AlFe phases, but AlFe phase-free regions were rarely observed. The inhibition of the flaky phases, combined with the blocky phases, on grain growth was greater than that in the AF1 alloy considering that the average length of the flaky phases in the AF15 alloy was significantly longer than the average diameter of the solid grains, enabling the grain coarsening of the AF15 alloy to be suppressed. Grain coarsening, which is the process of moving grain boundaries,[4,5] would cease only if boundary migration encountered an alloplastic barrier (such as the AlFe phase). The coarsening rate constants of the AF15 alloy were significantly lower than those of the AF1 alloy during isothermal heating; the AF15 alloy had only one-third to one-fifth of the coarsening rate constants of the AF1 alloy. This implies that Al-5Fe-4Cu-based alloys with lower coarsening rate constants would produce a large number of HAGBs due to the hindrance of the AlFe phases.

In addition, the grain boundaries in the initial microstructure of Al-5Fe-4Cu-based alloys played a key role in grain coarsening in the solid–liquid region. The fraction of AlFe phases in the AF15 alloy was approximately twice that of the AF1 alloy, and there were more complex morphologies, causing the grains with low disorientation boundaries to decrease and the agglomeration of grains to inhibit, because the AF15 alloy had more elements. The higher misorientation angles between grains could indirectly restrain the grain coarsening during heating in the solid–liquid region.[9] The role of AlFe phases in the inhibition of grain coarsening in Al-5Fe-4Cu-based alloys is similar to that of coarse silicon particles in thixoformed Al-Si-Mg alloy with a low liquid fraction,[10] Al_2Cu particles in 319 cast alloy,[8] or in cooling slope cast 2014 alloy[6,7] and the

7075 Al alloy with infusible nano-sized SiC particles,[24] which have very low coarsening rate constants during heating in the liquid–solid region. However, the inhibition of AlFe phases did not vary throughout the process, unlike the restraint effect of Si particles and Al_2Cu particles, which disappeared as the heating temperature increased or soaking time lengthened because of precipitation and dissolution,[6–8] indicating that the insoluble AlFe phases might provide a stronger restriction on solid grain coarsening.

CONCLUSION

During heating in the solid–liquid region, the average diameter of the grains in the Al-5Fe-4Cu-based alloys increased with elevating heating temperature and prolonged holding time, and the grains in the AF15 alloy were smaller and rounder than those in the AF1 alloy. Grain coarsening of the alloys followed the classic LSW theory at $n = 4$, a grain boundary diffusion-controlled coarsening, and the coarsening rate constant K first increased rapidly and then gently with increased holding time, and an inflection point appeared after isothermal heating for 20 min. The coarsening rate constants of the AF15 alloy were approximately one-fifth and one tenth those of the AF1 alloy in the earlier stage of heating (5–20 min) and in the later stage of heating (20–60 min), respectively. The infusible AlFe phases in the alloys deterred not only the development of solid grains, but also liquid convection, diffusion and merging. This mechanical restriction was always effective throughout heating in the solid–liquid region, and it promoted the formation of HAGBs. The mechanical barriers and the grains with more high-angle grain boundaries during heating in the solid–liquid region were the reason why the alloys had smaller coarsening rate constants and grain sizes. In particular, the AF15 alloy, whose fraction and morphology of AlFe phases were more complex than those in the AF1 alloy, enabled the formation of more barriers, prompting more grains with HAGBs to be generated.

ACKNOWLEDGEMENTS

The corresponding author, Bo Liu, would like to thank the Zhejiang Ocean University for research start-up funds (No. 21045012513). Thanks are due to Dr. Xiaojiao Zuo (Shenyang University of Technology) for taking some metallographic photos and to Professor Fen Zhang (Zhejiang Ocean University) for her assistance with refining the language.

ELECTRONIC SUPPLEMENTARY MATERIAL

The online version of this article (https://doi.org/10.1007/s11837-020-04338-7) contains supplementary material, which is available to authorized users.

REFERENCES

1. X.G. Yuan, S.G. Zhao, S. Li, Y.J. Lu, and H.J. Huang, *Foundry* 55, 466 (2006).
2. B. Liu, X.G. Yuan, and H.J. Huang, *China Foundry* 8, 424 (2011).
3. S.G. Zhao, *Study on semi-solid forming process of Al-Si-Fe alloy*, Dissertation, Shenyang University of Technology, Shenyang, 2009.
4. S. Annavarapu and R.D. Doherty, *Acta Metal. Mater.* 43, 3207 (1995).
5. E.D. Manson-Whitton, I.C. Stone, J.R. Jones, P.S. Grant, and B. Cantor, *Acta Mater.* 50, 2517 (2002).
6. H.V. Atkinson and D. Liu, *Mater. Sci. Eng. A* 496, 439 (2008).
7. H.V. Atkinson and D. Liu, *Trans. Nonferrous Met. Soc. China* 20, 1672 (2010).
8. K. Liu and X. Grant Chen, *Phys. B Condens. Matter* 560, 126 (2019).
9. K. Wang, Z.M. Zhang, H. Wen, D. Xia, and W.J. Sun, *Mater. Charact.* 121, 1 (2016).
10. A.M. Kliauga and M. Ferrante, *Acta Mater.* 53, 345 (2005).
11. H.T. Jiang and M.Q. Li, *J. Mater. Eng. Perform.* 13, 488 (2004).
12. T.J. Chen, Y. Hao, and J. Sun, *Mater. Sci. Eng. A* 337, 73 (2002).
13. F.R. Cao, R.G. Guan, L.Q. Chen, Z.Y. Zhao, and Y. Ren, *Chin. J. Nonferrous met.* 22, 7 (2012).
14. S.C. Wang, Y.Y. Li, W.P. Chen, and X.P. Zheng, *Trans. Nonferrous Met. Soc. China* 18, 784 (2008).
15. H. Mohammadi, M. Ketabchi, and A. Kalaki, *J. Mater. Eng. Perform.* 20, 1256 (2011).
16. A. Bolouri, M. Shahmiri, and C.G. Kang, *J. Mater. Sci.* 47, 3544 (2012).
17. B. Liu, X.G. Yuan, H.J. Huang, and Z.Q. Guo, *JOM* 64, 316 (2012).
18. B. Liu, X.G. Yuan, S.H. Zhang, and H.J. Huang, *J. Plast. Eng.* 16, 11 (2009).
19. X.G. Yuan, S.H. Zhang, B. Liu, and H.J. Huang, *J. Mech. Eng.* 46, 85 (2010).
20. J. Jiang, Y. Wang, J. Qu, Z. Du, Y. Sun, and S. Luo, *J. Alloys Compd.* 497, 62 (2010).
21. J. Jiang, Y. Wang, and H.V. Atkinson, *Mater. Charact.* 90, 52 (2014).
22. F.J. Humphreys and M. Hatherly, *Recrystallization and Related Annealing Phenomena* (Oxford: Pergamon Press, 1995).
23. Y.B. Yu, P.Y. Song, and S.S. Kim, *Scr. Mater.* 41, 767 (1999).
24. J.F. Jiang, Y. Wang, X. Nie, and G.F. Xiao, *Mater. Des.* 96, 36 (2016).